

RELIABILITY PERFORMANCE OF WIRELESS SENSOR NETWORKS FOR CIVIL INFRASTRUCTURE – PART II: PREDICTION AND VERIFICATION

Sun-Chan BAE^a, Won-Suk JANG^a, Mirosław J. SKIBNIEWSKI^{b, c}

^a*Department of Civil Engineering, Yeungnam University, 214-1 Dae-Dong Gyeongsan, Gyeongbuk 712-749, South Korea*

^b*Department of Civil and Environmental Engineering, University of Maryland, College Park, MD 20742, USA*

^c*Institute of Theoretical and Applied Informatics, ul. Bałycka 5, 44-100 Gliwice, Poland*

Received 23 Sep 2013; accepted 03 Jun 2014

Abstract. Application studies on wireless sensor networks (WSN) are actively conducted in the construction industry. However, there are several technical limitations including signal interference caused by the characteristics of wireless sensors, reliability degradation in wireless communication and uncertainty of configuring a network topology. This may lead to a decline in reliability and performance of real-time data acquisition methods. Thus, the paper developed a model capable of predicting reliability performance of wireless signals applied to civil infrastructures. The measured and predicted values of wireless signals are compared and analyzed through a field experiment carried out in an actual bridge to verify the prediction model suggested herein. As a result of the analysis, the prediction model demonstrated a variation up to 8.4% compared with actual measurements, proving the high accuracy of the prediction model. Furthermore, the reception rate at short distances within a 5 m radius is at least 90%, showing a highly reliable reception capacity. When this is applied to monitoring systems in the construction sector, it is believed that performance and reliability of such system can be secured.

Keywords: communication reliability, wireless sensor network, prediction, path loss, civil infrastructure.

Introduction

Recently ubiquitousness, implying something that exists anywhere, anytime, is being noticed at industry sectors. In this ubiquitous era, there is great interest on automated construction systems to enhance users' convenience and efficiency as buildings keep getting higher, larger and more complicated. Until now, the amount of logistics or manpower input has been identified manually at construction sites, and it was highly time-consuming to collect measurement data at construction sites. These have led to issues on unnecessary costs and low efficiency. Introduction of wireless communication has been accelerated to resolve such issues.

Various types of wireless communication technologies are applied to a wide range of areas. Yet, methods to accurately predict the performance of wireless communication have been limited despite the fact that reliable data collection is required at relatively large-scale areas like construction sites. This not only generates errors in measurement data and degrades reception reliability, but also reduces stability and efficiency of the network configuration. Ultimately, it may lead to direct loss in terms of system efficiency and reliability which are essential

in building wireless monitoring and tracking systems for civil infrastructure such as bridges and buildings. Therefore, the paper quantitatively analyzes various failure factors that are likely to affect wireless communications at construction sites. Also, it is intended to develop and verify a prediction model capable of identifying reliability performance of 2.4 GHz wireless communication by utilizing information on obstacle types, thickness and distance between sensors.

1. Literature review

The adoption of ZigBee as WSN technology has grown in many industrial applications responding to recent trends of remote sensing and wireless monitoring. In the civil and construction engineering areas, infrastructure monitoring, such as tunnels, dams, bridges, buildings, and highways, ZigBee is being used as the main driver of wireless data collection (Kim *et al.* 2011; Dhivya, Hemalatha 2013; Iqbal, Yukimatsu 2011; Miao *et al.* 2012; Kim *et al.* 2008; Dibley *et al.* 2012). Construction asset tracking, crew monitoring, safety monitoring and equipment tracking are other examples of ZigBee technology

Corresponding author: Mirosław J. Skibniewski
E-mail: mirek@umd.edu; mskibniewski@gmail.com

in construction engineering areas (Wu *et al.* 2013; Yang *et al.* 2011; Naticchia *et al.* 2013; Song *et al.* 2007). Some other ZigBee applications for data collection and processing also include underground monitoring, environmental monitoring, industrial control and monitoring, and localization (Sung, Tsai 2011; Xu, Wu 2012; Blumenthal *et al.* 2007; Hwang, Yu 2012). Although WSN technologies provide many opportunities and potential in data communication due to mobility and removal of wires, research on WSN is still in early stages with limited practical standards and applicability. In this respect, some researchers have pointed out the current challenges and raised issues regarding reliability, performance, network scalability, power management and fault tolerance (Jardosh, Ranjan 2008; Capella *et al.* 2005; Yick *et al.* 2008).

Performance reliability is one of the concerns of potential users of wireless technology in civil engineering applications. Basically, customers of civil infrastructure systems expect a similar level of performance reliability to that experienced in traditional wired systems (Silva *et al.* 2012). In a civil engineering sense, performance reliability means that the desired data is sent to the receiver at long distances with minimal measurement errors, as well as high data quality and delivery rate (Hwang *et al.* 2010). On the other hand, propagation of the radio signal through air often encounters coverage loss and deterioration of the link quality (Li *et al.* 2008). More complications lie in the fact that different radio frequencies, transmission power, obstruction type, and interference affect RF (Radio Frequency) propagation characteristics (Yick *et al.* 2008). RF propagation with a path loss model in indoor or outdoor environments has been the subject of extensive research in many wireless communities. The focus of research methods has mainly been on the theoretical waveguide model, site-specific statistical approaches, ray-tracing model, numerical model using finite difference time domain, and heuristic approaches (Sarkar *et al.* 2003). Nevertheless, the complexity of those methodologies and research outcomes do not completely provide practical implications to civil engineers who plan to adopt wireless sensor networks. In addition, such propagation environments are classified mainly by the building type, geometry of rooms and floors, and partitions. On the other hand, the unique characteristics of individual obstructions according to materials type and thickness have not been addressed. A broad classification of obstruction details and impractical guideline of WSN performance fail to provide a clear understanding of the WSN application framework to civil engineers.

Therefore, the methodology presented in this paper (including both parts I and II) aims to provide both experimental results and a prediction model to easily identify the performance reliability of WSN in civil infrastructure applications.

2. Path loss model

The log-distance path loss model is a generalized path loss model based on the free space path model which is

applied with the pass loss exponent n where values can be applied depending on the environmental conditions. The following equation can be deducted (Rappaport 2002):

$$PL(d)[dB] = PL(d_0) + 10n \log\left(\frac{d}{d_0}\right), \quad (1)$$

where: $PL(d)$ refers to the log-distance path loss and d_0 refers to the reference distance. Various values can be applied to the path loss exponent depending on the environmental settings. The path loss gets larger as the path loss exponent n increases as shown in Table 1.

Table 1. Path loss exponent, n , according to different environments (Rappaport 2002)

Environment	Path loss exponent, n
Free Space	2
Urban area cellular radio	2.7 to 3.5
Shadowed urban cellular radio	3 to 5
In building Line-Of-Sight	1.6 to 1.8
Obstructed in building	4 to 6
Obstructed in factories	2 to 3

Meanwhile, even if the distance between the transmitter and receiver is the same under the actual wireless environment, each path may have a different path loss according to the location of the receiving module and environment. However, these factors are not specifically reflected in the free space propagation model and the log-distance path loss model described above. Log-normal shadowing model is the model that reflects these factors, and it can be expressed as the following equation:

$$PL(d)[dB] = \overline{PL}(d) + X_\sigma = \overline{PL}(d_0) + 10n \log\left(\frac{d}{d_0}\right) + X_\sigma, \quad (2)$$

where: X_σ refers to the Gaussian random variable with standard deviation of σ with average 0. Eqn (2) reflects the random shadowing effect so that a different path loss can be generated on the same distance. In other words, even though the distance between the transmitter and receiver is the same, a different path loss can be generated depending on the surrounding environment, representing the shadowing effect. Here, shadowing implies that the radio wave that is diffracted, refracted and penetrated can reach the receiver again even if the module is blocked by an obstacle that causes interference in propagation.

The Okumura model is widely used to predict wireless signals at urban environments (Okumura *et al.* 1968). This model is mainly used at a frequency band of 150 MHz~1920 MHz, cell radius of 1 km~100 km and base station (BS) antenna height of 30 m~1000 m. The free space propagation model of Okumura $PL_{OK}(d)$ can be represented as the following equation:

$$PL_{OK}(d)[dB] = PL_F + A_M(f, d) - G_{Rx} - G_{Tx} + G_{AREA}, \quad (3)$$

where: $A_M(f, d)$ represents the average attenuation of means for the free space, G_{Rx} and G_{Tx} the transmitting antenna gain and the receiving antenna gain respectively and G_{AREA} the gain according to propagation environment. G_{Rx} and G_{Tx} consider only the effect of antenna height. Other factors such as the antenna pattern are not taken into consideration.

Currently, the most widely used path loss model is the Hata model which was based on the Okumura model (Hata 1980). Hata has performed modeling for large cities, suburban areas and open rural areas based on the Okumura's empirical path loss model. The path loss model at city areas can be represented as shown in Eqn (4):

$$PL_{Hata,U}(d)[dB] = 69.55 + 26.16 \log f_c - 13.82 \log h_{Tx} - C_{Rx} + (44.9 - 6.55 \log h_{Tx}) \log d, \quad (4)$$

where: f_c is the valid frequency at range of 150 MHz~1500 MHz, d is the T-R (Transmitter and Receiver) separation distance (km), the distance between the transmitter and receiver, and h_{Tx} is the height of transmitting antenna (m). C_{Rx} is the correlation coefficient of the receiving antenna, and there are 2 types according to the service propagation range. C_{Rx} for transmission at narrow transmitting/receiving range can be defined as shown in Eqn (5) and C_{Rx} for transmission at broad transmitting/receiving range as shown in Eqn (6):

$$C_{Rx} = 0.8 + (1.1 \log f_c - 0.7) h_{Rx} - 1.56 \log f_c; \quad (5)$$

$$C_{Rx} = \begin{cases} 8.29(\log(1.54h_{Rx}))^2 - 1.1, & \text{if } f_c \leq 200 \text{ MHz} \\ 3.2(\log(11.75h_{Rx}))^2 - 4.97, & \text{if } f_c > 200 \text{ MHz} \end{cases} \quad (6)$$

Meanwhile, the path loss model for suburban and open rural areas can be represented as $PL_{hata,SU}(d)$ and $PL_{hata,O}(d)$ respectively as shown in Eqns (7) and (8). The path loss is larger at urban areas with packed obstacles than at those with fewer obstacles:

$$PL_{Hata,SU}(d)[dB] = PL_{Hata,U}(d) - 2 \left(\log \frac{f_c}{28} \right)^2 - 5.4; \quad (7)$$

$$PL_{Hata,O}(d)[dB] = PL_{Hata,U}(d) - 4.78(\log f_c)^2 + 18.33 \log f_c - 40.97. \quad (8)$$

3. WSN prediction model for civil infrastructure

There have been multiple studies on empirical analyses, basically in the electrical and communications sectors,

to predict wireless communication just like the path loss model specified above (Sarkar *et al.* 2003). The referenced model is used to predict the reception performance of wireless signals at long-distance wireless communication networks by simplifying the attenuation effect of wireless signals on terrains or artificial structures. However, it is difficult to theoretically suggest the effect of attenuation taking into account the existence of obstacles at construction sites. The reason is that various types of obstacles are spread out at the site interfering with propagation, making it more complicated to identify the performance of wireless communication. Empirical analysis and quantitative prediction of wireless communications reliability under such environment may become highly-significant technical factors in improving the overall WSN system performance. Thus, this study developed a performance prediction model for wireless signals using regression analysis, based on the result of empirical experiments (refer to Part I) on the attenuation of wireless signal performance using concrete blocks and steel plates among representative construction materials. Three RSSI, LQI and PDR indexes have been adopted for the analysis (refer to Part I): RSSI (Received Signal Strength Index) is an indicator of power measurement calculated by the receiver; LQI (Link Quality Index) is an indicator to assess quality of the communication link between nodes; and PDR (Packet Delivery Rate) is defined as the ratio of the number of successfully received packets and transmitted packets.

In this paper, the path loss model is referred to as a theoretical background to formulate the empirical equations and development of the prediction model. Prediction of RSSI is based on the path loss model described as a log function. While predictions of LQI and PDR are not directly related to the path loss model, they are inferred as power functions from both the nonlinearity of the path loss model and experimental results in Part I.

3.1. Empirical equation

Concrete is an insulator with a dielectric constant of around 2.1–2.3 (water is 80.1 at 20 °C), so when a wireless signal penetrates concrete, some energy is reflected and the other is penetrated. Generally, the bigger the dielectric constant, more energy is reflected and absorbed and there is less radio wave penetration. In addition, even if materials have the same dielectric constant, the thicker the wireless signal, the less the radio wave penetrates. Penetration performance is likely to change depending on the homogeneity of material. Thus, reinforced concrete may have complicated patterns when it comes to radio wave penetration.

Quantitative analysis of experiments on wireless signal performance considering characteristics of concrete blocks was conducted in Part I. The concrete block used was plain with thickness ranging from 12–60 cm to obtain 3 different indexes (RSSI, LQI and PDR) per unit distance. The measured indexes per unit distance were then plotted in regression curves. The receiving patterns

by material thickness and T-R separation distance were analyzed to be used as reference data of the prediction model. Based on the regression curves of raw data, Table 2 demonstrates the empirical equations of RSSI, LQI and PDR expressed as log and power functions. Here, “a” and “b”, used as the equation coefficients, are functions of thickness t , where the thickness and characteristics of concrete block are taken into consideration. The calculation is explained in detail in the next section.

Table 2. Empirical equations for concrete block (x denotes T-R separation distance)

Thickness [m]	RSSI		LQI		PDR	
	$y = a \ln x + b$		$y = ax^b + 100$		$y = ax^b + 100$	
	a	b	a	b	a	b
12	-6.11	-63.35	-0.09	1.55	-1.4E-04	3.12
24	-5.75	-65.24	-0.18	1.41	-0.0035	2.42
36	-5.39	-67.14	-0.30	1.33	-0.021	2.02
48	-5.03	-69.03	-0.43	1.27	-0.085	1.73
60	-4.67	-70.93	-0.56	1.23	-0.251	1.51

Steel is a conductor with wave penetration properties that are very different from that of concrete. When a wireless signal hits a steel object, most of the electromagnetic field energy is reflected and only very little energy penetrates. So, if a steel plate is placed at the T-R path, only very little energy penetrates, resulting in a dramatic decline in received signal strength and reduction of link coverage. Likewise, based on the regression curves of raw data in Part I, Table 3 demonstrates the empirical equations of RSSI, LQI and PDR expressed as log and power functions. Here, “a” and “b”, used as the equation coefficients, are functions of thickness t of steel plate.

3.2. Signal prediction model using extended regression function (ERF)

The regression curves of the empirical equation described in the previous section are the log function for RSSI and power function for LQI and PDR, and each coefficient “a” and “b” is used. Since the coefficients applied herein

represent different characteristics according the material properties and thickness, it requires additional statistical analyses reflected with the values per measurement index and per material. Thus, this study intends to suggest a methodology for general users to predict approximate RSSI, LQI and PDR values using those empirical equations. This can be easily achieved by only calculating the coefficients based on the T-R separation distance and the thickness and material characteristics of the obstacles in order to build a network using wireless sensors. To do so, an extended regression function (ERF), in which the thickness of obstacles applied to the previously mentioned empirical equation is expanded, is deducted, and coefficients “a” and “b” according to the obstacle characteristics are applied to ERF. This methodology will be helpful to easily and efficiently predict the performance of wireless communication without executing a time-consuming reliability test for each node when building a network with hundreds and thousands of wireless sensor nodes.

Based on measurement data from 1 concrete block (12 m) – 5 concrete blocks (60 cm), and steel plates from 1 sheet (1 cm) – 10 sheets (10 cm), coefficients “a” and “b” per thickness were obtained for RSSI, LQI and PDR respectively. Thickness of the concrete block was then extended up to 180 cm and steel plate up to 20 cm to calculate RSSI, LQI, and PDR. The regression curves of coefficients “a” and “b”, where thickness is the independent variable, are shown in Figure 1. Coefficients “a” and “b” of the concrete block and steel plate for RSSI can be expressed linearly as they get thicker, yet there is a difference in “a” and “b” values according to the insulator and conductor characteristics. On the other hand, the regression curve of coefficients “a” and “b” for LQI and PDR shows a decreasing power function as the material gets thicker. A list of coefficient functions for each measurement index based on the characteristics of materials is specified in Table 4.

Based on the coefficient functions, a prediction model using ERF with different thicknesses from 12 cm up to 180 cm for concrete blocks and 1 cm to 20 cm for steel

Table 3. Empirical equations for steel plate (x denotes T-R separation distance)

Thickness [m]	RSSI		LQI		PDR	
	$y = a \ln x + b$		$y = ax^b + 100$		$y = ax^b + 100$	
	a	b	a	b	a	b
1	-6.11	-65.75	-0.019	2.05	-0.06	1.9
2	-6.02	-66.8	-0.06	1.8	-0.16	1.69
3	-5.93	-67.85	-0.12	1.66	-0.28	1.57
4	-5.84	-68.9	-0.24	1.56	-0.45	1.48
5	-5.75	-69.95	-0.4	1.48	-0.75	1.41
6	-5.66	-71	-0.6	1.42	-1.2	1.36
7	-5.57	-72.05	-1	1.36	-1.7	1.31
8	-5.48	-73.1	-1.5	1.32	-2.3	1.27
9	-5.39	-74.15	-2	1.28	-3.5	1.24
10	-5.3	-75.2	-3	1.24	-5	1.2

Table 4. List of coefficient functions for measurement index in each material type

		$a(t)$ Function	$b(t)$ Function
RSSI	Concrete Block	$0.03t - 6.47$	$-0.158t - 61.45$
	Steel Plate	$0.09t - 6.2$	$-1.05t - 64.7$
LQI	Concrete Block	$-0.08847\exp(0.0314t)$	$-0.2\ln(t) + 2.0458$
	Steel Plate	$-0.001789t/3.208 - 0.0554$	$-0.351\ln(t) + 2.0469$
PDR	Concrete Block	$-5.585e^{-010t/4.866} - 0.0002192$	$-\ln(t) + 5.603$
	Steel Plate	$-0.002809t/3.229 - 0.1644$	$-0.3028\ln(t) + 1.9$

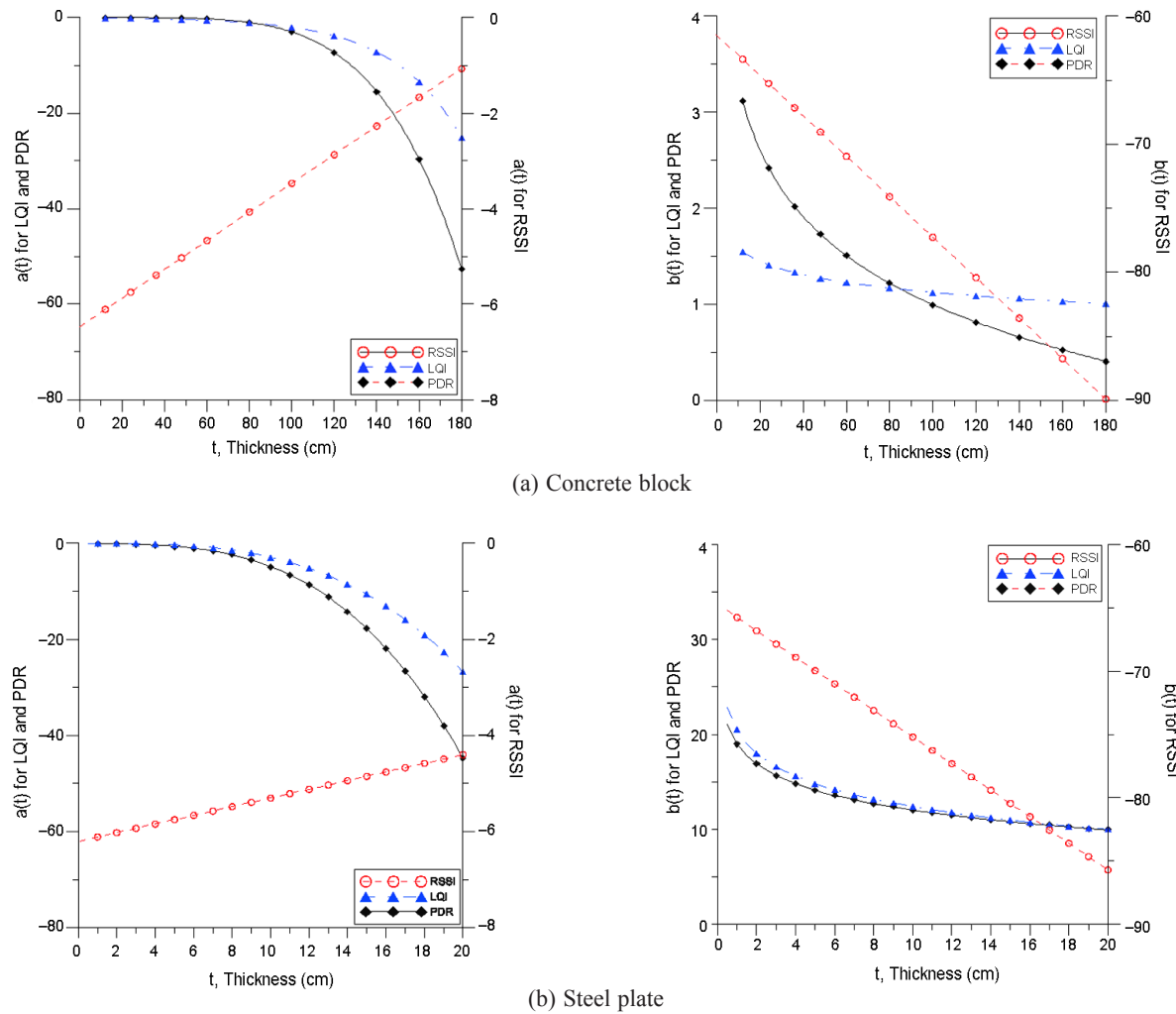


Fig. 1. Regression curve of Coefficient Functions $a(t)$ and $b(t)$

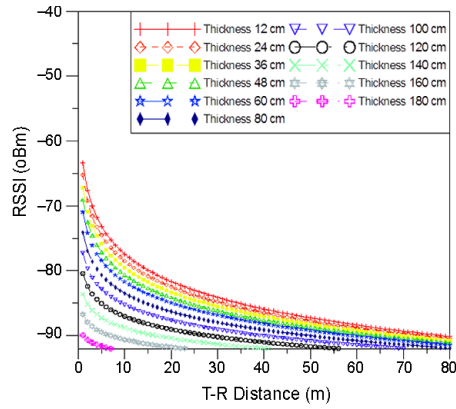
plates is suggested, and it is shown in Figures 2 and 3. It should be considered that coefficient functions “ a ” and “ b ” used at ERF are material thickness-dependent functions, so the coefficient that corresponds to material thickness should be chosen from Table 4 to be applied to ERF. Thus, a user can easily decide the prediction model at each T-R separation distance by applying the empirical equations with the values of coefficients “ a ” and “ b ”. It is interesting to note that the reception coverage distance slightly varies according to the measurement index in the prediction model. This is because occasional packet reception at the receiver was found even under -90 dBm yet LQI and PDR values are very low. Thus, reception coverage distances of LQI and PDR become slightly shorter than that of RSSI at the regression curve equation.

4. Verification of prediction model based on case study

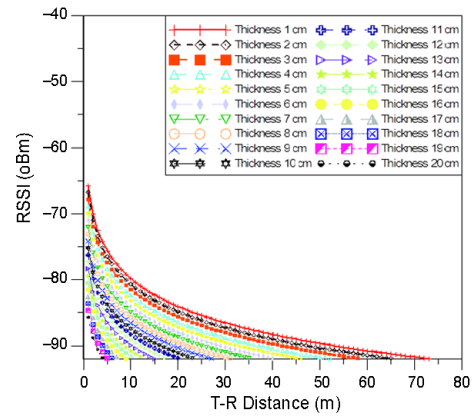
This section is intended to perform verification on the reliability of the prediction model by comparing and analyzing the index values measured and calculated from the representative bridges with real wireless sensors attached. To do so, the shape of the actual bridge girder,

the thickness of the obstacle penetration on the T-R path and the T-R separation distance between transmitters and a receiver were calculated. Then, the measured values and predicted values of RSSI, LQI and PDR under the same conditions were compared and analyzed. In addition, measured values and predicted values were interpolated and visually represented using a contour map for verification. Figure 4 illustrates details of a concrete and steel box girder bridges. For the concrete girder bridge, the thickness of the longitudinal and lateral girder is 31 cm and 20 cm, respectively. For the steel box girder bridge, the thickness of the box web is 1cm and flange length of the box is 238 cm.

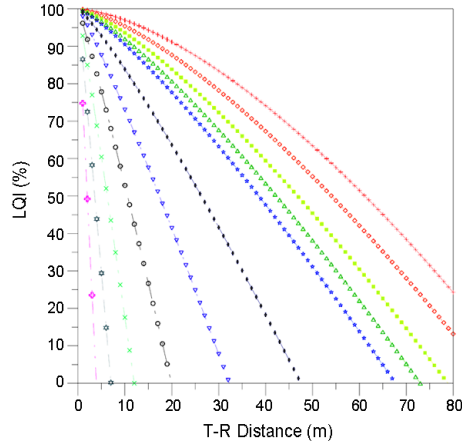
For verification analysis: 1) 24–32 ZigBee nodes were attached to the center of longitudinal girders, transmitting the 2.4 GHz RF packet at intervals of 1 Hz to the base station (BS) node, and the RSSI, LQI and PDR at the BS were measured; 2) assuming that the same sensor nodes are attached to the girder of the same study bridge, the information on the penetration thickness of girder existing on T-R path is applied. Then, the corresponding information is inserted as an ERF variable to calculate predicted values of RSSI, LQI and PDR.



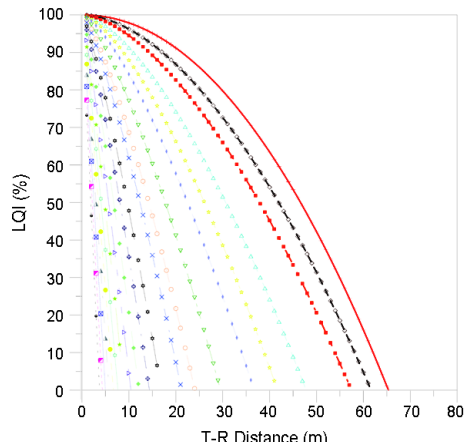
(a) RSSI



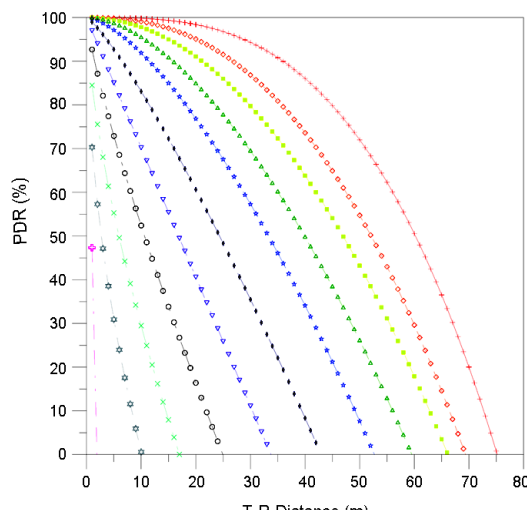
(a) RSSI



(b) LQI

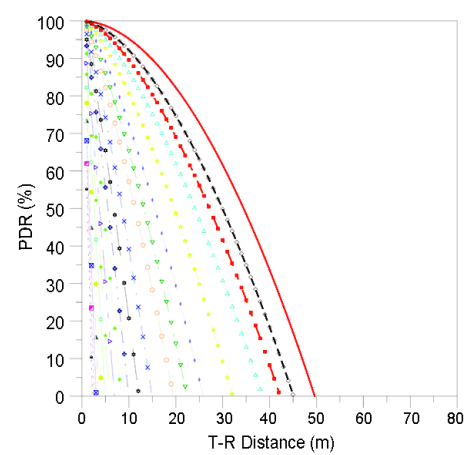


(b) LQI



(c) PDR

Fig. 2. Extended regression function (ERF) for concrete block



(c) PDR

Fig. 3. Extended regression function (ERF) for steel plate

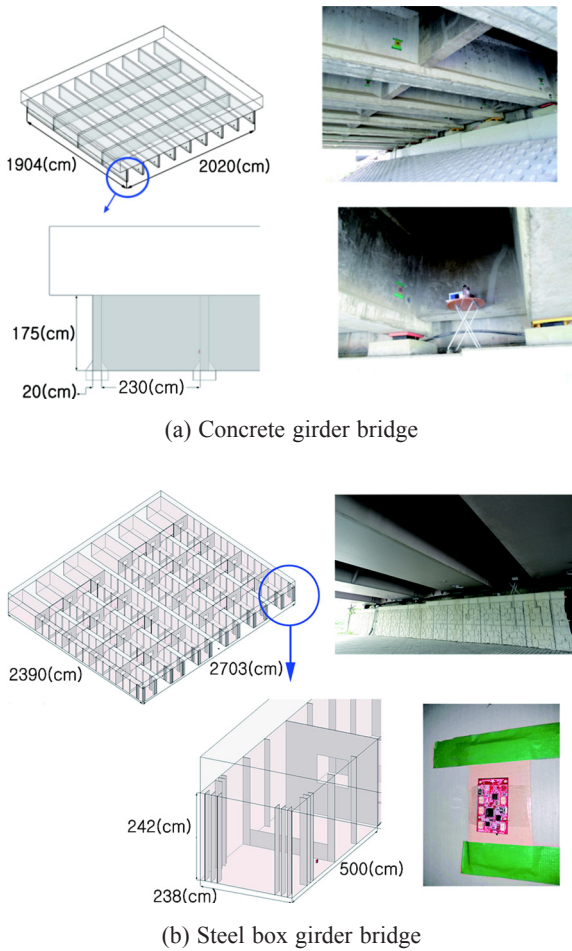


Fig. 4. Detail drawings of each bridge type

4.1. Concrete girder bridge

The first experiment was carried out at Apryang Bridge, a concrete girder bridge situated in Gyeongsangbuk-do, South Korea. As shown in Figure 5, 24 sensors were attached to the girder and RF packets were to be sent to the BS located in the center.

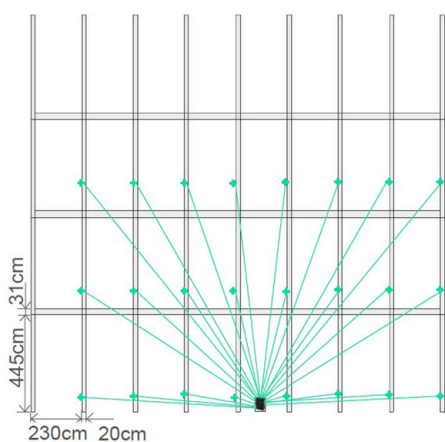


Fig. 5. Distribution of sensor nodes in concrete girder bridge (BS is placed at bottom center)

Figure 6 demonstrates measured and predicted values obtained for each evaluation index with the BS at center of the concrete girder bridge. In the RSSI case, both measured and predicted values show a relatively concentric circular distribution, yet when it comes to LQI and PDR, a shallower distribution toward a longitudinal direction is shown. Since the antenna of the ZigBee module is omnidirectional, a concentric circular distribution is likely if the T-R path is on a line-of-sight (LOS) without obstacles. However, varying contour map distributions may be generated depending on the distribution of obstacles at the T-R path where the signal is blocked by the girders as shown in the experiment. Moreover, if the distance from the BS is within 5 m, measured values and the predicted values of the evaluation indexes are relatively similar, yet the T-R separation distance gets longer, slightly different distribution patterns are displayed. This implies that there may be unpredictable influencing factors as the girder where wireless signals penetration gets thicker and the T-R separation distance gets longer. This may be owing to the interference of multipath or irregular reinforcement status, yet its effect may be insignificant.

Among the three evaluation indexes, the one that may have practical meaning to construction engineers is

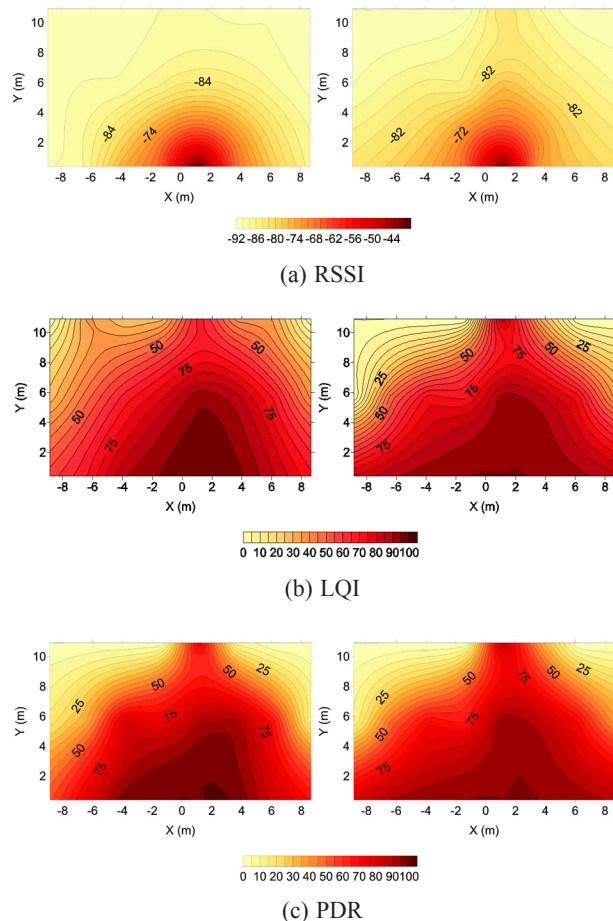


Fig. 6. Contour map for concrete girder bridge with BS at center (left: measured and right: predicted map)

PDR which is the ratio of packets received out of total transmitted packets. According to Figure 6(c), the contour distribution of measured and predicted values within a 5 m radius represents a PDR of 95% or higher, indicating that it is a zone where reliability is secured when building a wireless sensor network system. Although the PDR range with secured reliability may vary according to the applied areas, a zone with at least 95% reception rate is at the permissible reliability zone when considering the general monitoring level.

4.2. Steel box girder bridge

The second experiment was performed at a steel box girder bridge called Yeonho Bridge located in Daegu, South Korea. A total of 32 sensors were attached in a box, which were set for transmission to the central BS (Fig. 7).

Figure 8 demonstrates the measured and predicted values obtained for each evaluation index with the BS at center of the steel box girder bridge. In the figure, both the measured and predicted values show a relatively concentric circular distribution, displaying relatively similar distribution patterns of measured and predicted values at the same location. Similar to the experiment on the concrete bridge, when it comes to PDR, in which general wireless sensor users like construction engineers are more interested, values measured and predicted within a 5 m radius show highly reliable values of at least 90% in average. This indicates that communication reliability is superior under a 5 m T-R separation distance when applied for general monitoring of the site.

Unlike the concrete bridge results, the measured and predicted values of the steel girder bridge were slightly different. This is believed to be resulting from the uncertainty of wireless signals that show highly varying reception performance according to peripheral conditions even where static wireless communications are carried out at the same distance and location. Moreover, since 32 wireless sensor modules were installed in a steel box, it is likely that various types of multipath such as refraction and reflection exist, and such atypical distribution of measured values is caused by electromagnetic characteristics inside the steel box. Despite all this, the distribution of measure-

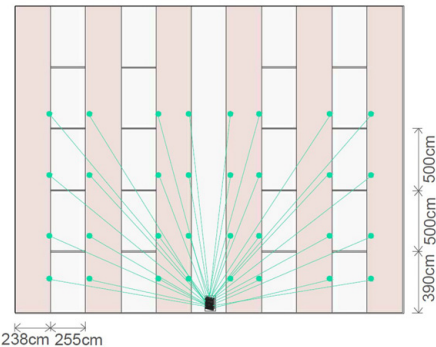


Fig. 7. Distribution of sensor nodes in steel box girder bridge (BS is placed at bottom center)

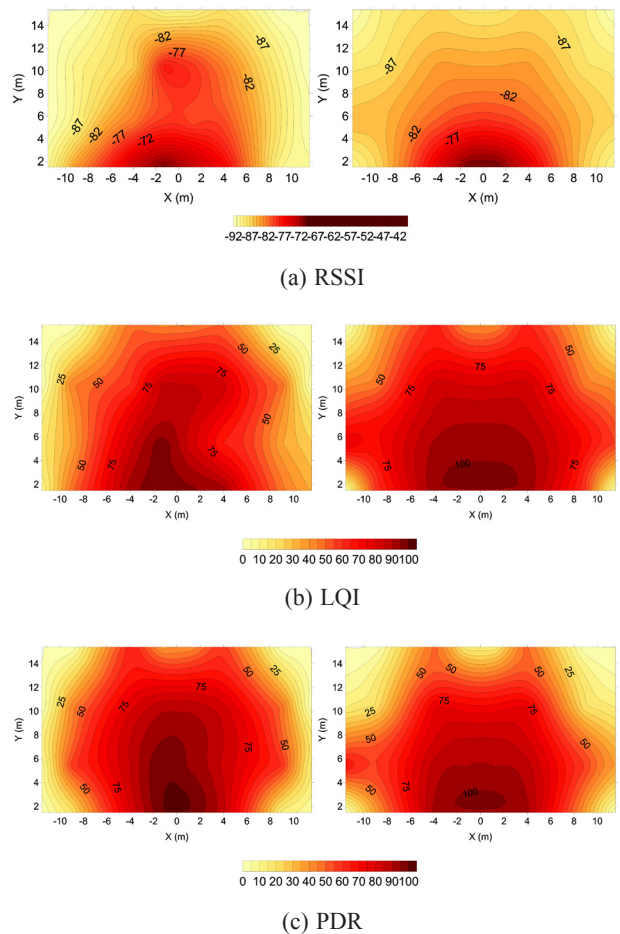


Fig. 8. Contour map for steel box girder bridge with the BS at center (left: measured and right: predicted map)

ment and prediction values within a 5 m radius is very similar in the contour map.

To verify the accuracy of the prediction model, deviation of measured and predicted values at each point where a concentric circle and a straight line meets were compared and analyzed as shown in Figure 9. The performance evaluation index at the point where the concentric circle and the straight line meet is not the actual measured value but the value interpolated by the contour map representing the evaluation index value extracted from a random location. This can propose a random evaluation method on the accuracy of the actual measurement and the prediction model. Here, the thickness of obstacles refers to the actual penetration thickness considering the incident angle and the number of girders. In addition, the deviation values of measurement and prediction are represented in percentage taking into account the full range of each evaluation index. In other words, it represents the error between measured and predicted values (in percentage) at the full span of 0 dBm and -92 dBm in case of RSSI, and the error between the measured and the predicted values at full span of 100% and 0% in case of LQI and PDR.

As shown in Figure 10, average deviation values of three evaluation indexes received from each sensor arranged in the same concentric circle are marked on the left

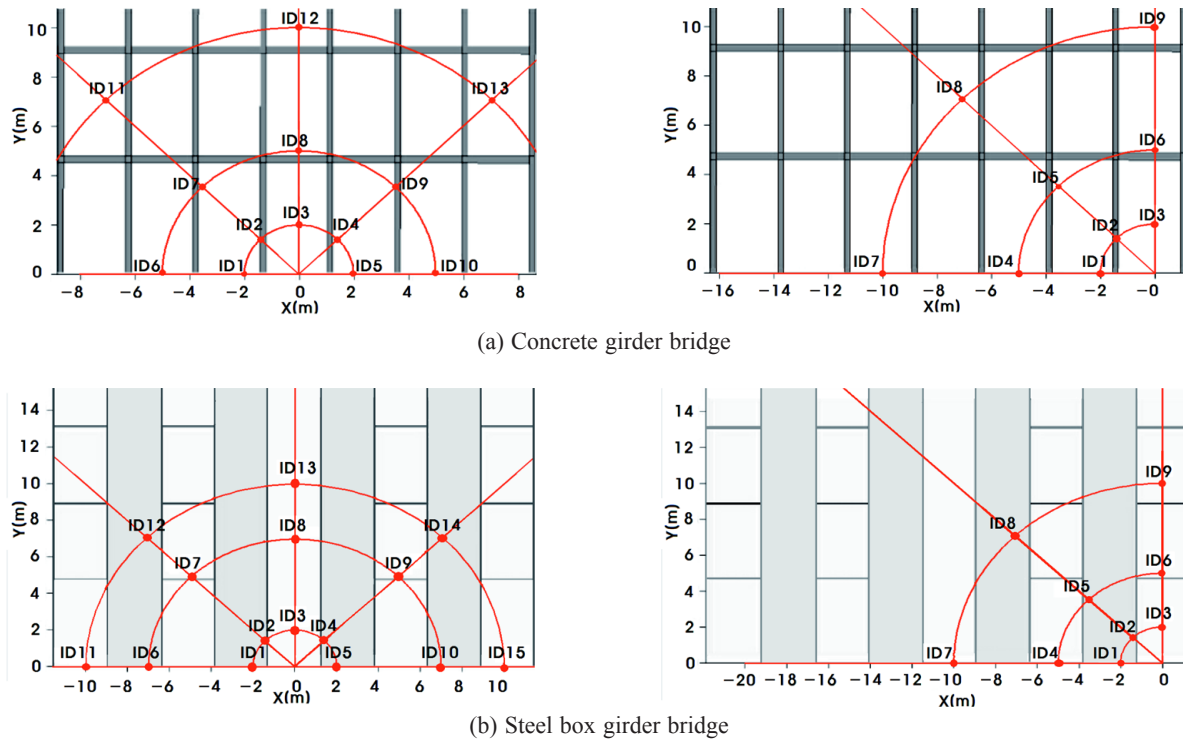


Fig. 9. Selection of random measurement points in each bridge (left: BS at center; and right: BS at corner)

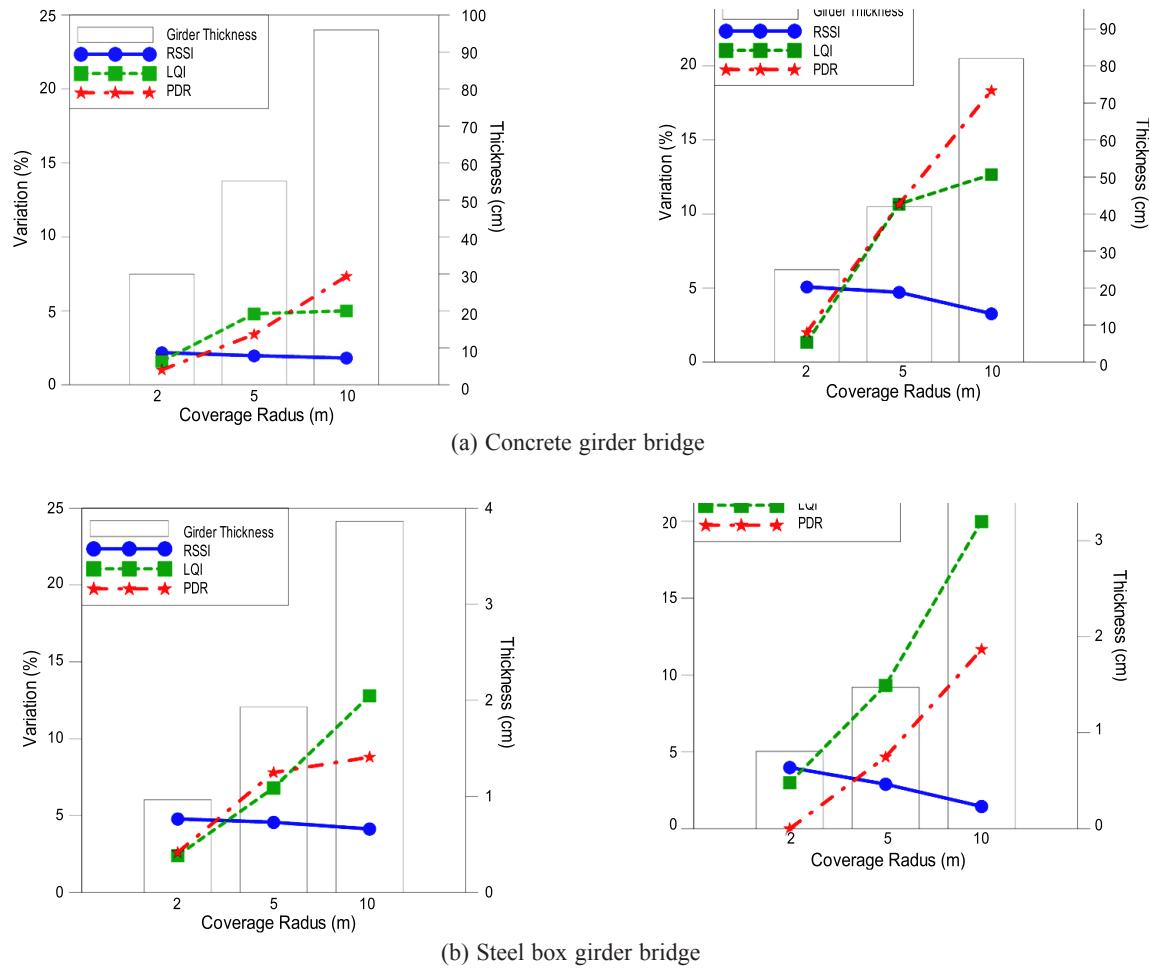


Fig. 10. Variation between measurement and prediction in each radius (left: BS at center; and right: BS at corner)

y-axis. Also, the actual penetration thickness of obstacles placed at the T-R path is displayed on the right y-axis, with the location of the BS distinguished as center and right corner for the concrete girder and the steel box girder bridge. The average deviation of all 4 cases is 3.4% for RSSI, 7.5% for LQI and 6.5% for PDR, verifying that the accuracy of the proposed prediction model is excellent as the error of all reception performance indexes is within 8%. When analyzing the respective evaluation index, the deviation slightly decreases as the T-R radius increases in case of RSSI. This is easily acceptable when considering the RSSI curve per T-R separation distance (refer to Fig. 2a). RSSI value dramatically decreases at a short-distance zone and as the distance gets longer, it converges around -90 dBm. Thus, fluctuation of the received signal at short distances is bigger than that at longer distances.

In the case of LQI and PDR, deviation values increase as the T-R separation distance and the thickness of obstacles increase. The measured raw data of LQI and PDR gradually decrease as the T-R separation distance and the actual penetration thickness increase, and drastically increase at the long distance zone (refer to Figs 2b and 2c). Thus, the zone where LQI and PDR changes are drastic shows a bigger deviation of measurement values per unit distance. It is believed that additional environmental factors including multipath may impact the reception performance under low signal strength. There is another result to pay attention to. The average penetration thickness of a concrete girder bridge and a steel box girder bridge is 55.0 cm and 2.1 cm respectively and even though the value of actual penetration thickness of the steel box girder bridge is very small, each reception performance at both girder bridges is similar. It can be inferred that the propagation interference of steel materials is far greater than that of concrete under the same concentric radius.

Conclusions and discussion

The study proposes a model to predict the performance of wireless communication using the least possible information such as obstacles, material characteristics and thickness, and T-R separation distance. With the lab experiment results, the study suggests a prediction model applied to the extended regression function (ERF) of RSSI, LQI and PDR by type and thickness of obstacles using regression analysis method. In addition, the model was verified by comparing and analyzing measured and predicted values from actual experiments in the selected concrete and steel girder bridges.

The prediction model showed very similarly patterned distributions with the actual measurement in 3 performance indexes while demonstrating a slight difference owing to uncertainty factors such as multipath. As represented in the error analysis, the deviation between measured and the predicted values gets bigger when the T-R distance increases. However, at least 90% of PDR is shown within a 5 m radius, demonstrating high reliability. Errors of 4.4%, 7.8%, and 8.4% were deducted

in RSSI, LQI, and PDR, respectively when measured and predicted values were compared. While short coverage for higher reliability is a generic limitation of low-power ZigBee devices, extension of network coverage can be possibly achieved by adopting a multihop network scheme for WSN applications in large-scale civil infrastructure. It was verified that the proposed prediction model is highly accurate. If the prediction model is interconnected with 3D design tools such as BIM in the near future, it is anticipated that a highly efficient and reliable network topology design can be achieved at the construction design phase taking into consideration attenuation of wireless signals.

The presented methodology and results are one of the few approaches to explore WSN performance in civil infrastructure. Therefore, analysis on WSN accuracy performance from the prediction model compared with field experiments would provide academic and practical contribution to the application of WSN bridge monitoring.

Acknowledgements

This research was supported by Senior Research Program through the National Research Foundation of Korea (NRF) grant funded by the Ministry of Education, Science and Technology (NRF-2012R1A2A2A02003265).

References

- Blumenthal, J.; Grossmann, R.; Golatowski, F.; Timmermann, D. 2007. Weighted centroid localization in Zigbee-based sensor networks, in *Proc. of IEEE International Symposium on Intelligent Signal Processing*, 3–5 October 2007, Alcala de Henares, Spain, 1–6.
- Capella, J. V.; Ors, R.; Bonastre, A.; Serrano, J. J. 2005. New challenges in wireless sensor networks: fault tolerance and real time, in *Proc. of IEEE International Conference on Industrial Technology*, 14–17 December 2005, Hong Kong, 1385–1390.
- Dhivya, A.; Hemalatha, M. 2013. Structural health monitoring system – an embedded sensor approach, *International Journal of Engineering and Technology* 5(1): 273–281.
- Dibley, M.; Li, H.; Rezgui, Y.; Miles, J. 2012. An ontology framework for intelligent sensor-based building monitoring, *Automation in Construction* 28: 1–14.
<http://dx.doi.org/10.1016/j.autcon.2012.05.018>
- Hata, M. 1980. Empirical formula for propagation loss in land mobile radio services, *IEEE Transactions on Vehicular Technology* 29(3): 317–325.
<http://dx.doi.org/10.1109/T-VT.1980.23859>
- Hwang, K. I.; Choi, B. J.; Kang, S. H. 2010. Enhanced self-configuration scheme for a robust ZigBee-based home automation, *IEEE Transactions on Consumer Electronics* 56(2): 583–590. <http://dx.doi.org/10.1109/TCE.2010.5505974>
- Hwang, S.; Yu, D. 2012. Remote monitoring and controlling system based on ZigBee networks, *International Journal of Software Engineering and Its Application* 6(3): 35–42.
- Iqbal, R.; Yukimatsu, K. 2011. Intelligent transportation systems using short range wireless technologies, *Journal of Transportation Technologies* 1(4): 132–137.
<http://dx.doi.org/10.4236/jtts.2011.14017>
- Jardosh, S.; Ranjan, P. 2008. A survey: topology control for wireless sensor networks, in *Proc. of IEEE International conference on Signal Processing, Communications and Networking*, 4–6 January 2008, Chennai, India, 422–427.

- Kim, J. R.; Yoo, H. S.; Kwon, S. W.; Cho, M. Y. 2008. Integrated tunnel monitoring system using wireless automated data collection technology, in *Proc. of the 25th International Symposium on Automation and Robotics in Construction (ISARC2008)*, 26–29 June 2008, Vilnius, Lithuania, 337–342.
- Kim, J.; Lynch, J. P.; Lee, J. J.; Lee, C. G. 2011. Truck-based mobile wireless sensor networks for the experimental observation of vehicle-bridge interaction, *Smart Materials and Structures* 20(6): 1–14.
<http://dx.doi.org/10.1088/0964-1726/20/6/065009>
- Li, Y.; Song, Y. Q.; Schott, R.; Wang, Z.; Sun, Y. 2008. Impact of link unreliability and asymmetry on the quality of connectivity in large-scale sensor networks, *Sensors* 8(10): 6674–6691. <http://dx.doi.org/10.3390/s8106674>
- Miao, X.; Chu, J.; Zhang, L.; Qiao, J. 2012. Development of wireless sensor network for dam monitoring, *Journal of Information & Computational Science* 9(6): 1609–1616.
- Naticchia, B.; Vaccarini, M.; Carborari, A. 2013. A monitoring system for real-time interference control on large construction sites, *Automation in Construction* 29: 148–160.
<http://dx.doi.org/10.1016/j.autcon.2012.09.016>
- Okumura, T.; Ohmori, E.; Fukuda, K. 1968. Field strength and its variability in VHF and UHF land-mobile radio service, *Review Electrical Communication Laboratory* 16(9–10): 825–873.
- Rappaport, T. S. 2002. *Wireless communications: principles and practice*. 2nd ed. Upper Saddle River, NJ, USA: Prentice Hall TPR. 736 p.
- Sarkar, T. K.; Ji, Z.; Kim, K.; Medouri, A.; Salazar-Palma, M. 2003. A survey of various propagation models for mobile communication, *IEEE Antennas and Propagation Magazine* 45(3): 51–82.
<http://dx.doi.org/10.1109/MAP.2003.1232163>
- Silva, I.; Guedes, L. A.; Portugal, P.; Vasques, F. 2012. Reliability and availability evaluation of wireless sensor networks for industrial applications, *Sensors* 12(1): 806–838.
<http://dx.doi.org/10.3390/s120100806>
- Song, J. H.; Lee, N. S.; Yoon, S. W.; Kwon, S. W.; Chin, S.; Kim, Y. S. 2007. Material tracking for construction logistics, in *Proc. of the 24th International Symposium on Automation & Robotics in Construction (ISARC2007)*, 19–21 September 2007, Madras, India, 63–67.
- Sung, W. T.; Tsai, M. H. 2011. Multi-sensor wireless signal aggregation for environmental monitoring system via multi-bit data fusion, *Applied Mathematics and Information Sciences* 5(3): 589–603.
- Wu, W.; Yang, H.; Li, Q.; Chew, D. 2013. An integrated information management model for proactive prevention of struck-by-falling-object accidents on construction sites, *Automation in Construction* 34: 67–74.
<http://dx.doi.org/10.1016/j.autcon.2012.10.010>
- Xu, H.; Wu, J. 2012. Metal mine underground safety monitoring system based on WSN, in *Proc. of the 9th IEEE International Conference on Networking, Sensing and Control*, 11–14 April 2012, Beijing, China, 244–249.
- Yang, X.; Lu, C.; Pan, W. 2011. A ZigBee-based highway vehicles prevent collision warning system research, in *Proc. of the Fourth International Symposium on Computational Intelligence and Design (ISCID11)*, 28–30 October 2011, Washington, DC, USA, 270–273.
- Yick, J.; Biswanath, M.; Ghosal, D. 2008. Wireless sensor network survey, *Computer Networks* 52(12): 2292–2330.
<http://dx.doi.org/10.1016/j.comnet.2008.04.002>

Sun-Chan BAE. Mr, Graduate Research Assistant, PhD Candidate in the Department of Civil Engineering, College of Engineering at Yeungnam University, South Korea. Member of Korean Society of Civil Engineers (KSCE) and Korea Institute of Construction Engineering and Management (KICEM). His research interests include the application of wireless sensor network applications to the performance monitoring of construction equipment, crews and materials.

Won-Suk JANG. Dr (deceased), Assistant Professor in the Department of Civil Engineering, College of Engineering at Yeungnam University, South Korea. Member of Korean Society of Civil Engineers (KSCE), Korea Institute of Construction Engineering and Management (KICEM), Korean Society of Ubiquitous Monitoring (KSUM), and Korean Institute of Building Information Modeling (KIBIM). His research interests included IT-based Civil and Infrastructure Engineering and Management, such as applications of wireless sensor networks, web-based project management systems, construction assets tracking, and building information modeling.

Miroslaw J. SKIBNIEWSKI. Dr, Professor of Construction Engineering and Project Management at the University of Maryland in College Park, USA. An author or coauthor of over 250 publications, he is a member of American Society of Civil Engineers (ASCE); a founding member, co-director and past president of International Association for Automation and Robotics in Construction (IAARC); and a past affiliate of International Council for Building Research Studies and Documentation (CIB). His current research interests include information technology support for infrastructure resilience, construction automation and robotics, information technology in construction management, e-commerce technology applications in construction, and green intelligent buildings. Among Prof. Skibniewski's awards is an honorary doctorate from Vilnius Gediminas Technical University presented in 2009.